

Calculation of resistive spectrum of MHD modes in tokamak with small resistivity

B. Rahmani, Ahmad Salar Elahi*, M. Ghoraneviss

Physics Department, Science and Research Branch, Islamic Azad University, Tehran, Iran

(Communicated by Ehsan Kozegar)

Abstract

The Compressible MHD resistance equations were written for the IR T1 tokamak configuration with one or two singular surfaces for density mass profiles. And they are linearized around equilibrium state. The eigenvalues and eigen functions of the resistive MHD modes were obtained for poloidal and toroidal mode numbers numerically by Mathematica software for homogeneity and in homogeneity plasma. The values obtained show that the eigenvalues are complex, and they are placed on certain curves. Also by drawing a diagram of eigen functions, it was determined that they were damped.

Keywords: Tokamak, MHD Spectra, Resistive Spectrum
2020 MSC: 35P30, 00A69

1 Introduction

For the understanding of ideal and resistive Magnetohydrodynamic MHD plasma phenomena such as heating, stability, study of linearized motion has significantly provided. The most total picture is gotten by means of a normal-mode analysis [4, 8, 9]. Since the analysis is entirely difficult both analytically and numerically. Simpler methods have been expanded. Knowledge of the ideal problem was used to expand a spectral code of solving for the complete spectra of compressible resistive MHD. By using of Mathematica software discretization leads the general complex eigenvalue problem $Ax \equiv \lambda Bx$. Inverse vector iteration, which keeps the band structure of the matrices, discovers selected eigenvalues and allows total parts of the complex spectrum to be continually arranged even in cases of large matrix dimension. This plan is suited to analyzing the complex resistive spectrum. The resistant MHD equations are not self-adjoint and the ideal spectrum which is a continuous spectrum completely, is removed and damped waves appear. Using the analysis of cylindrical geometry, complex eigenvalues were obtained which are located on certain curves. We study the resistive Alfvén modes in detail for experimentally relevant configurations. Our numerical scheme yields an accuracy resulting in much finer details of the spectrum. Complete results can thus be given. It is found that the ideal continua disappear and are approximated only at the end points and a few selected interior points. The interior points are present in terms of the ideal Alfvén dispersion relation $\omega_A \equiv |k \cdot B_0| / \sqrt{\rho_0}$, where k is wave vector of the perturbation and B_0 the equilibrium magnetic field; ρ_0 is the density. Configurations with magnetic shear and with one or two resonant surfaces in the plasma are treated. The eigenvalues locate on specific curves in the complex plane which become independent of resistivity. In this fusion the spectrum is arranged completely for

*Corresponding author

Email address: salari_phy@yahoo.com (Ahmad Salar Elahi)

configurations where three or four branch points are involved in the eigenvalue curves [5, 6, 8]. In this paper, we examine the subtle structure of the resistance spectrum to obtain results in internal Alfvén modes in order to find an effective mechanism that is highly desirable in a variety of ways with Mathematica software. In previous papers [4, 5] the spectrum obtained is for constant mass density. While in this work, we have used variable mass density. The paper was organized as follows: the physical model which is the common compressible resistive MHD model was presented in the section 2 and the results for different type of density, for tokamak like equilibria with singular surface $k.B_0 = 0$ for $m = 1, 2, 3$ were obtained. Then the case with two resonant surfaces in the plasma was discussed in section 3 and finally the discussions are in section 4.

2 Simulation Method

Since in the plasma, the ensemble of particles exhibit collective behavior, it can be defined in terms of single fluid theory. In the tokamak device a toroidal current in the plasma generates a poloidal magnetic field. This poloidal field with the toroidal field, come equilibrium and heats the plasma. The resistance magnetohydrodynamic equations study in normalized, dimensionless form consists of [4]:

1. equation of motion:

$$\rho \left(\frac{\partial \vec{V}}{\partial t} + V \cdot \nabla V \right) = -\nabla P + (\nabla \times B) \times B, \quad (2.1)$$

2. Maxwell-Ohm:

$$\frac{\partial B}{\partial t} = \nabla \times (V \times B) - \nabla \times (\eta \nabla \times B), \quad (2.2)$$

3. Adiabatic law:

$$\frac{\partial P}{\partial t} = -\gamma P \nabla \cdot V - V \cdot \nabla P, \quad (2.3)$$

4. Maxwell:

$$\nabla \cdot B = 0. \quad (2.4)$$

where B the magnetic field, V velocity of the fluid, P the pressure, ρ the mass density, η is the resistivity, γ is the ratio of the specific heats. Physical quantities are normalized using the characteristic length L , which is the same as the scale of Alfvénic units, a characteristic magnetic field strength B_0 , and a characteristic density ρ_0 . Velocities are then presented in terms of the Alfvén speed $V_A \equiv B_0 / \sqrt{\mu_0 \rho_0}$, time in terms of $\tau_A = L / V_A$. Notice that the supposition of incompressibility $\nabla \cdot V = 0$ is not made [3, 6, 8]. If the pressure variations are small compared with the mean thermodynamic pressure, the incompressible equations of motion accurately indicate the plasma behavior. Since the resistive modes rapidly oscillate, the compressible set of equations is appropriate. Since the dissipation proportional to η is considered to be small, the adiabatic law is adopted for the equation of state. At this point these equations become linear around a static equilibrium denoted by $\partial/\partial t = 0$. And $V_0 = 0$. The equilibrium is then defined by the equation [2].

$$\nabla P_0 = (\nabla \times B_0) \times B_0 \quad (2.5)$$

We use a cylindrical symmetry approximation to calculate the resistive spectrum, because an IR-T1 tokamak has inverse aspect ratio $a/R_0 = 12.5/45 = 0.27$ [9-10] and a circular cross section. In straight geometry static, ideal equilibria can be interpreted as resistive equilibria if $\nabla \times \eta(\nabla \times B_0) = 0$, with the consequence that $\eta_0 j_0 = E_z = \text{const}$. In toroidal geometry a resistive equilibrium is only possible with flow. i.e. $V_0 = 0$. It is proportional to η and hence very small. Here we take the simplest approach of a constant resistivity η_0 instead constant E_z . This simplification does not establish any restriction on unstable modes, since the resistivity decouples the magnetic field from the fluid in localized regions where the perturbation corresponds the field. But also the results for stable modes are only insignificantly modified by using constant resistivity. The equilibrium quantities for a cylindrical symmetry only have an r -dependence. With the usual cylindrical coordinates r, θ, z the equilibrium is determined by the following equation [2]:

$$\frac{\partial P_0}{\partial r} = -\frac{1}{r} B_\theta \frac{\partial}{\partial r} (r B_\theta) - B_z \frac{\partial}{\partial r} B_z. \quad (2.6)$$

With two profiles, and solving the Eq. (2.6), the last profile can be obtained. Equilibrium profiles in plasma boundary conditions are selected so that the safety factor from $q_0 = 2$ on axis to $q_1 = 4$. The perturbations from the equilibrium are follows:

$$\begin{aligned} V(r, t) &= v(r, t) \\ B(r, t) &= B_0(r, t) + b(r, t) \\ P(r, t) &= P_0(r, t) + p(r, t) \end{aligned}$$

The following function is suitable for separating perturbed quantities:

$$f(r, \theta, z, t) = f(r) \exp(im\theta + ink + i\omega t), \quad (2.7)$$

where $f(r)$ is the amplitude of perturbation, ω is the Eigen frequency.

The growth rate $\lambda_r = Re(i\omega)$ is denoted as the real part of $\lambda = i\omega.n$ is the toroidal mode number, and m is related to the poloidal mode number. Finally $k = 2\pi/L$ explains a periodicity length. In ideal MHD λ is either real or purely imaginary, which cause to unstable or purely oscillating waves. By including resistance, the frequency can be complex. The equations for the perturbed quantities v , p and b are follows [4]:

$$i\omega\rho_0 v = -\nabla p + (\nabla \times B_0) \times b + (\nabla \times b) \times B_0, \quad (2.8)$$

$$i\omega p = -\gamma P_0 \nabla \cdot v - v \cdot \nabla P_0, \quad (2.9)$$

$$i\omega b = \nabla \times (v \times B_0) - \nabla \times (\eta \nabla \times b). \quad (2.10)$$

The perturbation resistance is considered to be zero, so the ripple mode is eliminated [4]:

$$i\omega\rho_0 \frac{v_1}{r} = -\left[\frac{\hat{P}}{r} + \frac{1}{m} B_\theta b'_1 + \left(B_z - \frac{1}{m} B_\theta \right) \frac{b_3}{r} \right]' + \frac{1}{r} \left(\frac{m}{r} B_\theta + nk B_z \right) b_1 - \frac{2}{rm} B_\theta b'_1 + \frac{2nk}{rm} B_\theta b_3. \quad (2.11)$$

$$i\omega\rho_0 r v_2 = \frac{m}{r} \hat{p} + \left(\frac{1}{r} B_\theta + B'_\theta \right) b_1 - \frac{nkr}{m} B_z b'_1 + \left(\frac{n^2 k^2 r}{m} + \frac{m}{r} \right) B_z b_3. \quad (2.12)$$

$$i\omega\rho_0 \frac{v_3}{r} = \frac{nk}{r} \hat{p} - \left(\frac{n^2 k^2}{m} + \frac{m}{r^2} \right) B_\theta b_3 + \frac{nk}{m} B_\theta b'_1 + B'_z \frac{1}{r} b_1. \quad (2.13)$$

$$i\omega \frac{\hat{p}}{r} = -\frac{1}{r} \hat{p}' v_1 - \gamma p_0 \frac{1}{r} v'_1 - \gamma p_0 \frac{m}{r} v_2 - \gamma p_0 \frac{nk}{r} v_3 \quad (2.14)$$

$$i\omega b_1 = -\left(\frac{m}{r} B_\theta + nk B_z \right) v_1 + \eta_0 \left[b''_1 + \frac{1}{r} b'_1 - \left(\frac{m^2}{r^2} + n^2 k^2 \right) b_1 - \frac{2nk}{r} b_3 \right]. \quad (2.15)$$

$$i\omega b_3 = -B_z v'_1 - m B_z v_2 + \frac{m}{r} B_\theta v_3 - B'_z v_1 + \eta_0 \left[\left(b'_3 - \frac{b_3}{r} \right)' + \frac{1}{r} b'_1 - \left(\frac{m^2}{r^2} + n^2 k^2 \right) b_3 \right]. \quad (2.16)$$

The variable changed to $v_1 = r v_r$, $v_2 = i v_\theta$, $v_3 = i r v_z$, $\hat{p} = r p_1$, $b_1 = i r b_r$, $b_3 = r b_z$. for preserve the Eq. (2.6) components $\{v_1, v_2, v_3, \hat{p}, b_1, b_3\}$ as real quantities [3, 4, 5, 6, 8]. The poloidal component $b_\theta \equiv b_2$ of the perturbed

b-field was eliminated by means of the divergence-free condition $\nabla \cdot b_1 = 0$, $-i/r(b_1' - mb_2 - nkb_3) = 0$ which will be obtained for poloidal modes, $m \neq 0$.

We now discuss the boundary conditions. Plasma is assumed to be surrounded by a perfectly conductive wall, which indicates the following conditions at the wall: $b_1(a) = 0$, $v_1(a) = 0$ and all quantities at the origin $r = 0$ are assumed to be known, $b_1(0) = 0$, $b_3(0) = 0$, $v_1(0) = 0$, $v_3(0) = 0$, $\hat{p}(0) = 0$. The eigenvalue problem of Eqs. (2.11),(2.12),(2.13),(2.14),(2.15),(2.16) obtains of a system of coupled ordinary differential equations (ODEs) which can be symbolically exhibited as $Ax \equiv \lambda Bx$ where λ is eigenvalue, and x is eigenvector, these are in general, complex. A is a general, non-Hermitian matrix and B is symmetric and positive certain.

Since in our problem A and B are real matrices, the eigenvalues appear in complex conjugate pairs.

3 Result

3.1 First approximate

A tokamak-like equilibria current density j , and constant toroidal field is given by

$$j_z = j + 0(1 - r^2/a^2)^2, \quad (3.1)$$

$$B_z = 1, \quad (3.2)$$

The plasma assumed to be homogeneous, so $\rho = 1$. For these profiles the safety factor, which is defined as usual as

$$q(r) = \frac{rkB_z(r)}{B_\theta(r)}. \quad (3.3)$$

$$q(r) = \frac{6k}{j_0[(r/a)^4 - 3(r/a)^2 + 3]}. \quad (3.4)$$

The ratio of on surface and on axis is $q(a)/q(0) = 3$. The constant j_0 in Eq (3.1) is used to vary $q(0)$ and is chosen such that the resonant surface is in the middle of the plasma; i.e. $q(0)$ with $q(r_s) = 2$ and $r_s = 0.5a$. By using of equation:

$$\begin{aligned} j_0 &= (\nabla \times B_0) \\ j_z &= \frac{1}{r} \frac{d}{dr}(rB_\theta) \end{aligned} \quad (3.5)$$

B_θ is fined. Then by using eq. (2.6) we calculate:

$$p_0 = j_0^2/6 \left[\frac{1}{10} \left[(1 - (r/a)^{10}) \right] - \frac{5}{8} \left[(1 - (r/a)^8) \right] + \frac{5}{3} \left[(1 - (r/a)^6) \right] - \frac{9}{4} \left[(1 - (r/a)^4) \right] - \frac{3}{2} \left[(1 - (r/a)^2) \right] \right] \quad (3.6)$$

Frequency of Alfven wave is [5]:

$$\begin{aligned} \omega_A(r) &= |k \cdot B_0| / \sqrt{\rho} \\ \omega_A(r) &= \left(\left(\frac{m}{r} \right) B_\theta + nkB_z \right) / \sqrt{\rho} \end{aligned} \quad (3.7)$$

The value j_0 is chosen such that the resonant surface is lies in the middle of the plasma which means that the wave vector of the perturbation is perpendicular to the magnetic field in that location, i.e. $F = k \cdot B_0|_{r=r_s} = 0$ with $q(r_s) = 2$ and $r_s = 0.5a$. and $k = 0.1$ [5]. To my concern, the problems related to non-hermitian operators don't have a unique approach. Direct or iterative methods can usually be chosen to solve large numerical systems. we apply of the

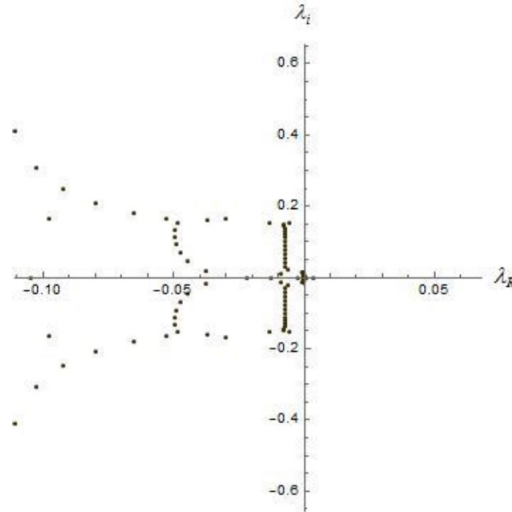


Figure 1: The Complete resistive spectrum for $j_z = j_0(1 - r^2/a^2)^2$, homogene plasma $\rho = 1$

Mathematica software for solving the resistive MHD equations. The eigenvalues and eigenvectors are obtained. The complex eigenvalues are exhibited in Fig. 1. λ_R represents the growth rate and λ_i represents the oscillation frequency.

The Alfvén mode spectra for $n = 1$ and $m = -2$ is showed in Fig. 2.

The sound mode spectrum is concentrated close to the origin and has a more complicated structure.

The sound modes are not well resolved at this scale and are therefore omitted from this and the following graphs.

Eigen functions corresponding to the respective modes in the branches have different numbers of radial oscillations. For a given branch, the number of oscillations from the endpoints on the imaginary axis increases until this number becomes infinite at the cumulative points corresponding to and $-\infty$ on the real axis [5]. By using eq. (3.7), $\omega_A(a) = 0.18$, that correspond with Fig. 2.

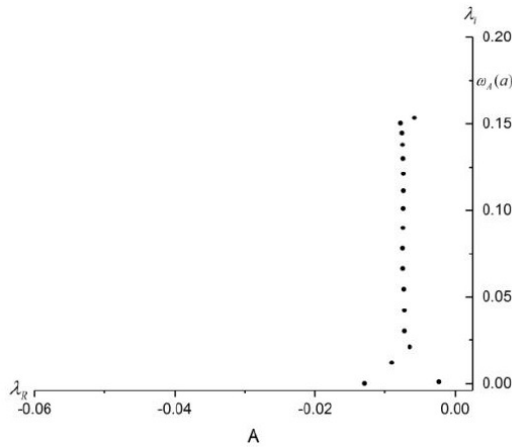


Figure 2: The resistive Alfvén spectrum for $j_z = j_0(1 - r^2/a^2)^2$, for $\rho = 1$, $\eta = 10^{-5}$, $n = 1$, $m = -2$.

In Fig. 3 for the perturbed field $b_1 = irb_r$ is displayed. This perturbation has a finite value at the singular surface. Perturbed velocity $v_1 = rv_r$, displayed in Fig. 4.

These, Normal components have a limited value at the singular surface.

In tokamak IR-T1 toroidal mode number and poloidal mode number are: $n = 1$, $m = 1$, $m = 2$, $m = 3$. Calculation is repeated for $m = -1$ and $m = -3$, so we set:

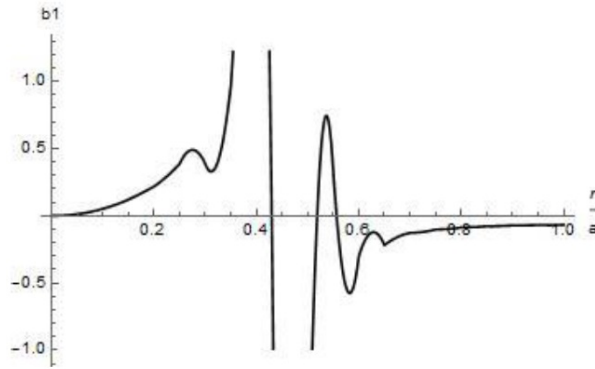


Figure 3: Normal component of the perturbed magnetic field $b_1 = irb_r$, with the singular surface at $r = 0.5a$.

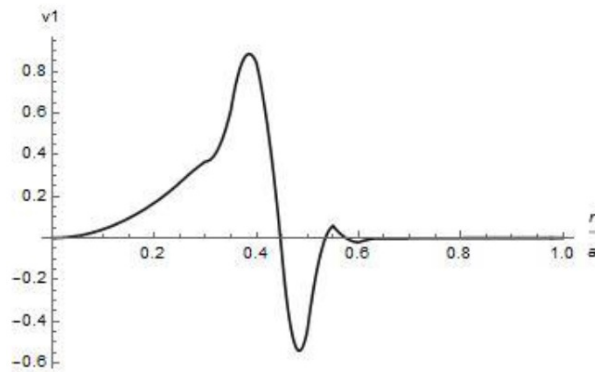


Figure 4: Normal component of the perturbed velocity $v_1 = rv_r$, with the singular surface at $r = 0.5a$.

$$j_z = j_0(1 - r^2/a^2)^2, \rho_0 = 1.$$

$$p_0 = j_0^2/6 \left[\frac{1}{10} [(1 - (r/a)^{10})] - \frac{5}{8} [(1 - (r/a)^8)] + \frac{5}{3} [(1 - (r/a)^6)] - \frac{9}{4} [(1 - (r/a)^4)] - \frac{3}{2} [(1 - (r/a)^2)] \right]$$

The eigenvalue distribution of the $m = -1$ and $m = -3$ modes are shown in Fig. 5 and Fig. 6 respectively.

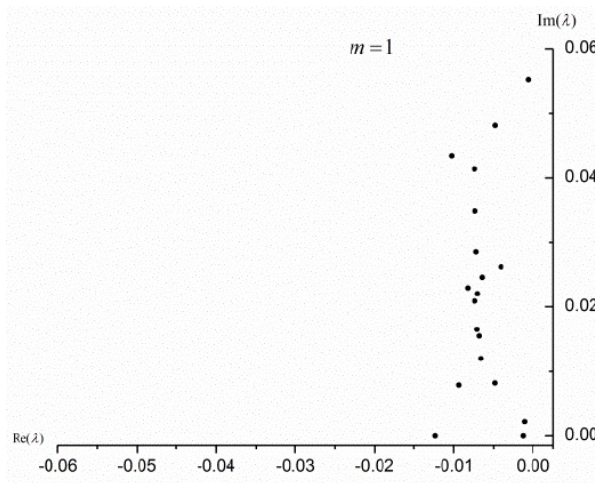


Figure 5: The resistive Alfvén spectrum for a tokamak-like current profile, homogeneous plasma for $\eta = 10^{-5}$, $n = 1$, $m = -1$, $k = 0.2$.

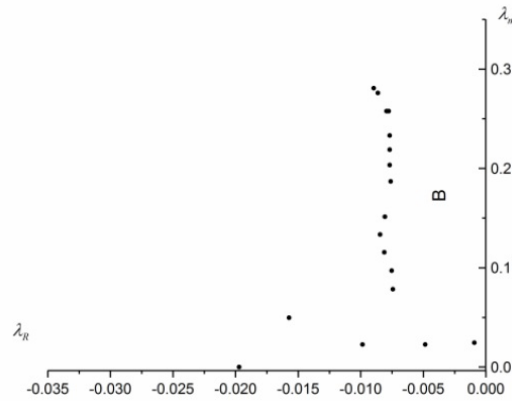


Figure 6: The resistive Alfvén spectrum for $j_z = j_0(1 - r^2/a^2)^2$, homogeneous plasma for $\eta = 10^{-5}$, $n = 1$, $m = -3$, $k = 0.2$.

3.2 Second approximate

We now consider configurations with two singular surfaces, such as occur in the building up phase of tokamaks and in hollow temperature and current profiles frequently watched. It is explained by

$$\begin{aligned}
 j_z &= j_0(1 + 10r^2/a^2)(1 - r^2/a^2)^3, \\
 B_z &= 1 \\
 \rho &= 1.
 \end{aligned}
 \tag{3.8}$$

For $q(0) = 2.5$ the singular surfaces are placed at $r/a = s_1 = 0.30$ and $r/a = s_2 = 0.73$. A pronounced dip happens at the center. The Alfvén frequency $\omega_A(r)$ has two zero transitions with a maximum in between at $r/a = r_e = 0.52$. By using equations (2.6) and (3.5) we read:

$$\begin{aligned}
 p_0 &= j_0^2/8 \left[2(1 - (r/a)^2) + \frac{21}{2}(1 - (r/a)^4) - \frac{23}{3}(1 - (r/a)^6) - \frac{485}{8}(1 - (r/a)^8) + \frac{1533}{10}(1 - (r/a)^{10}) \right. \\
 &\quad \left. - \frac{2023}{12}(1 - (r/a)^{12}) - \frac{1417}{14}(1 - (r/a)^{14}) - \frac{268}{8}(1 - (r/a)^{16}) + \frac{40}{9}(1 - (r/a)^{18}) \right]
 \end{aligned}
 \tag{3.9}$$

The resistive Alfvén spectrum for $k = 0.2$, $n = 1$, $m = -2$, $\eta = 10^{-5}$ is shown in Fig. 7 [4].

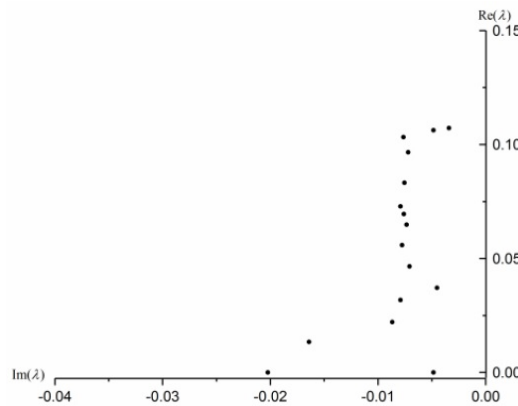


Figure 7: The resistive Alfvén spectrum for homogeneous plasma, $j_z = j_0(1 + 10r^2/a^2)(1 - r^2/a^2)^3$, $\eta = 10^{-5}$, $n = 1$, $m = -2$, $r/a = s_1 = 0.30$.

If plasma is considered inhomogeneous, density mass profile is [1].

$$\rho = \rho_0(1 - r^2/a^2)^\alpha \tag{3.10}$$

in Eq. (3.10) we choose $\alpha = 1$:

$$\begin{aligned} \rho &= \rho_0(1 - r^2/a^2), \quad \rho_0 = 1 \\ j_z &= j_0(1 + 10r^2/a^2)(1 - r^2/a^2)^3, \end{aligned}$$

For the pressure profile in Equation (3.9). The calculations are repeated and the complex eigenvalues are shown in Figure 8.

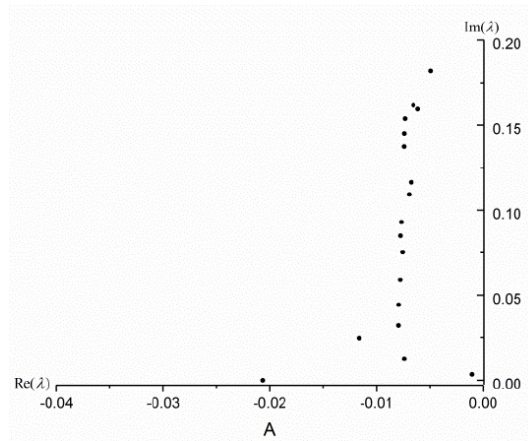


Figure 8: The Alfvén resistive spectrum for $j_z = j_0(1 + 10r^2/a^2)(1 - r^2/a^2)^3$, $\rho = \rho_0(1 - r^2/a^2)$, $\eta = 10^{-5}$, $n = 1$, $m = -2$, $k = 0.2$.

We set $\alpha = 2$, so:

$$\begin{aligned} \rho &= \rho_0(1 - r^2/a^2)^2, \quad \rho_0 = 1 \\ j_z &= j_0(1 + 10r^2/a^2)(1 - r^2/a^2)^3, \end{aligned}$$

The result was showed in Fig. 9:

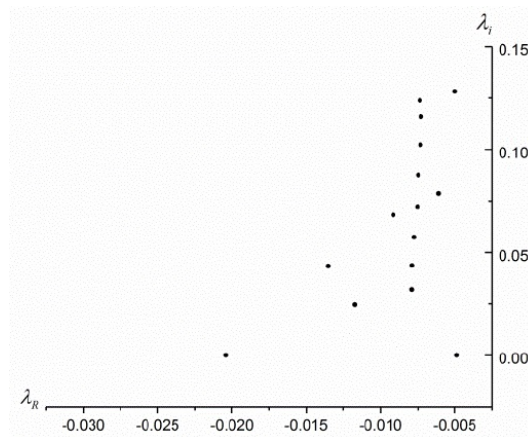


Figure 9: The Alfvén resistive spectrum for $j_z = j_0(1 + 10r^2/a^2)(1 - r^2/a^2)^3$, $\rho = \rho_0(1 - r^2/a^2)$, $\eta = 10^{-5}$, $n = 1$, $m = -2$, $k = 0.2$.

We choose the resistivity $\eta = 8 \times 10^{-6}$ and $\eta = 10^{-5}$. The calculates are repeated for $\rho = 1$, $j_z = j_0(1 + 10r^2/a^2)(1 - r^2/a^2)^3$, in Fig. 10 can be seen that in $\eta = 10^{-5}$ and $\eta = 9 \times 10^{-6}$ the points of the spectrum are on a specialized curve.

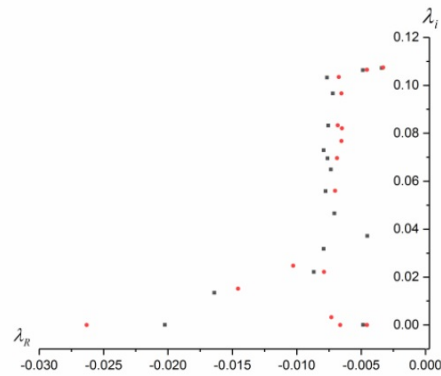


Figure 10: The resistive spectrum for $j_z = j_0(1 + 10r^2/a^2)(1 - r^2/a^2)^3$, with two singular surfaces for values of resistivity $\eta = 10^{-5}$ (black) and $\eta = 9 \times 10^{-6}$ (red).

4 Conclusions

To understand the MHD spectrum in the IR-T1 tokamak with cylindrical geometry of plasma for $m = 1$, $m = 2$ and $m = 3$ resistance MHD modes are investigated by solving an eigenvalue problem based on reduced MHD model. Resistance plasma column surrounded by a perfect conductor wall. We used numerical normal-mode analysis. the simulations were based on tokamak-like equilibrium profiles for, $B(r)$, $j_z = j_0(1 - r^2/a^2)^v$ and $q(r)$ on homogeneous plasma in the presence of the $n = 1$, $m = -2$ instability. We have used by Mathematica software for determination of eigenvalues and eigenfunctions. Spectrum is lied on especial curve. the results are consistent with other researches. Presence of the $n = 1$, $m = -2$ instability, Eigenfunctions $b_1(r)$ and $v_1(r)$ are displayed. These are damped. We repeat the calculation for $m = 1$ and $m = 3$. For tokamak-like equilibrium $j_z = j_0(1 + 10r^2/a^2)(1 - r^2/a^2)^3$, with two singular surfaces for homogeneous plasma and inhomogeneous plasma spectrum are obtained.

It can be seen that in $\eta = 10^{-5}$, $\eta = 9 \times 10^{-6}$ the spectrum points are on some curve. Our result agreement with other researches [1, 2, 3, 6, 7, 8, 10].

References

- [1] D. Chenna Reddy and T. Edlington, *Plasma density measurements on compass-c tokamak from electron cyclotron emission cutoffs*, Rev. Sci. Instrum. **67** (1996), no. 2, 462–468.
- [2] J.P. Freidberg, *Plasma physics and fusion energy*, Cambridge University Press, 2008.
- [3] J.P. Goedbloed, H.A. Holties, S. Poedts, G.T.A. Huysmans and W. Kerner, *MHD spectroscopy: free boundary modes (ELMs) and external excitation of TAE modes*, Plasma Phys. Control. Fusion **35** (1993), no. SB, p. B277.
- [4] W. Kerner, *Computing the complex eigenvalue spectrum for resistive magnetohydrodynamics*, Elsevier Sci. **127** (1986), 241–265.
- [5] W. Kerner, K. Lerbinger and K. Riedel, *Resistive Alfvén spectrum of tokamaklike configurations in straight cylindrical geometry*, Phys. Fluids, **29** (1986), no. 9, 2975–2987.
- [6] W. Kerner and H. Tasso, *Tearing mode stability for arbitrary current distribution*, Plasma Physics, **24** (1982), no. 1, p. 97.
- [7] T. Matsumoto and S. Tokuda, *Eigenvalue spectrum of MHD modes in cylindrical tokamak plasma with small resistivity*, Plasma Fusion Res. Ser. **9** (2010), 568–573.
- [8] E. Teller, *Fusion. Volume 1. Magnetic confinement. Part B*, Academic Press, 1981.
- [9] B. Van der Holst, A.J.C. Beliën, J.P. Goedbloed, M. Nool and A. Van der Ploeg, *Calculation of resistive magnetohydrodynamic spectra in tokamaks*, Phys. Plasmas **6** (1999), no. 5, 1554–1561.
- [10] A. Salar Elahi, M. Ghoranneviss, M. Emami and A. Rahimi Rad, *Theoretical and experimental approach in poloidal beta and internal inductance measurement on IR-T1 tokamak*, J. Fusion Energy **28** (2009), no. 4, 346–349.